Toxicology Letters 295 (2018) 179–186

Contents lists available at ScienceDirect

Toxicology Letters

journal homepage: www.elsevier.com/locate/toxlet

Inhibition of Nrf2 alters cell stress induced by chronic iron exposure in human proximal tubular epithelial cells

S.E.G. van Raaij[a], R. Masereeuw[b], D.W. Swinkels[a], R.P.L. van Swelm[a,*]

[a] Department of Laboratory Medicine, Radboud Institute for Molecular Life Sciences, Radboud University Medical Centre, Nijmegen, The Netherlands
[b] Division of Pharmacology, Utrecht Institute for Pharmaceutical Sciences, Utrecht University, Utrecht, The Netherlands

ARTICLE INFO

Keywords:
Iron overload
Oxidative stress
Nrf2
ER stress
Renal proximal tubular epithelial cell

ABSTRACT

Iron can catalyze reactive oxygen species (ROS) formation, causing cellular injury. In systemic iron overload, renal tubular epithelial cells are luminally exposed to high iron levels due to glomerular filtration of increased circulating iron. Reports of tubular dysfunction and iron deposition in β-thalassemia major support an association between increased chronic iron exposure and renal tubular injury. In acute iron exposure, Nuclear factor-erythroid 2-related factor 2 (Nrf2) may protect from iron-induced injury, whereas chronic renal stress may lead to Nrf2 exhaustion. We studied the cytotoxic mechanisms of chronic iron exposure using human conditionally immortalized proximal tubular epithelial cells (ciPTECs). Long-term iron exposure resulted in iron accumulation, cytosolic ROS formation and increased *heme oxygenase 1 (HMOX-1)* mRNA expression (all $p < 0.001$). This was accompanied by nuclear translocation of Nrf2 and induction of its target protein NQO1, which both could be blocked by the Nrf2 inhibitor trigonelline. Interestingly, iron and trigonelline incubation reduced ROS production, but did not affect *HMOX-1* mRNA levels. Moreover, ferritin protein and *CHOP* mRNA expression were induced in combined iron and trigonelline incubated cells ($p < 0.05$). Together, these findings suggest that chronic iron exposure induces oxidative stress and that exhaustion of the antioxidant Nrf2 pathway may lead to renal injury.

1. Introduction

Iron is indispensable for life, but it can also be harmful by catalyzing reactive oxygen species (ROS) formation in the Fenton reaction (Koppenol, 1993). The human body carefully regulates iron uptake and storage, but has limited abilities to regulate iron excretion (Brissot and Loreal, 2016). As a result, increased intestinal iron uptake in hereditary hemochromatosis and increased body iron acquisition through frequent red blood cell transfusions in β-thalassemia syndromes have been shown to result in chronic systemic iron overload and subsequent organ damage (Brissot and Loreal, 2016). Patients with systemic iron overload suffer from elevated circulating iron levels, which are bound to the transport protein transferrin (transferrin-bound iron, TBI) (Brissot and Loreal, 2016). Once transferrin becomes largely saturated with iron, non-transferrin-bound iron (NTBI) can be detected (Brissot et al., 2012; de Swart et al., 2016). Although iron is tightly bound to transferrin in TBI, iron is only loosely bound to small molecules such as citrate, in NTBI (Brissot et al., 2012). As such, iron in NTBI is available for redox cycling and is, therefore, considered a toxic iron species (Brissot et al., 2012; Cabantchik, 2014). Circulating TBI and NTBI are filtered into the renal tubular lumen by the glomerulus (Thevenod and Wolff, 2016; Zhang et al., 2007; Norden et al., 2001). Subsequently, iron in the tubular lumen is suggested to be completely reabsorbed by renal tubular cells, since hardly any iron is present in urine of healthy volunteers (Rodriguez and Diaz, 1995; Green et al., 1968). As a result, in patients with elevated circulating iron levels, proximal tubular epithelial cells (PTECs) are chronically exposed to high and potentially harmful iron levels.

In patients with hereditary hemochromatosis (Ozkurt et al., 2014; Marble and Bailey, 1951; Rous, 1918; Okumura et al., 2002; Chmieliauskas et al., 2017) or β-thalassemia major (ElAlfy et al., 2018; Hashemieh et al., 2017), renal iron deposition has been observed. Moreover, renal dysfunction in patients with β-thalassemia major has been reported with increased urinary excretion of N-acetyl-β-D-glucosaminidase (NAG) and β-2-microglobulin, both markers for renal PTEC damage (ElAlfy et al., 2018; Hashemieh et al., 2017; Annayev et al., 2018; Quinn et al., 2011; Ahmadzadeh et al., 2011; Deveci et al., 2016). Combined, these observations suggest that chronic iron overload may cause increased iron accumulation in the kidney, and, as such, may lead to clinically relevant nephrotoxicity over time.

* Corresponding author at: Department of Laboratory Medicine, Translational Metabolic Laboratory (830), Radboud University Medical Center, P.O. Box 9101, 6500 HB, Nijmegen, The Netherlands.
E-mail address: Rachel.vanSwelm@Radboudumc.nl (R.P.L. van Swelm).

https://doi.org/10.1016/j.toxlet.2018.06.1218
Received 15 May 2018; Received in revised form 18 June 2018; Accepted 26 June 2018
Available online 28 June 2018

The question remains, however, which exact molecular mechanisms are involved in renal tubular injury during chronic TBI and NTBI exposure. Previous animal and human studies suggest that chronically increased renal tubular iron exposure and injury in systemic iron overload depend on the balance between oxidative stress and anti-oxidative systems (Budak et al., 2014; Sponsel et al., 1996; Sheerin et al., 1999; Ansar et al., 2014; Gholampour et al., 2017; von Herbay et al., 1994; Ghone et al., 2008). The major cellular pathway that protects against oxidative injury has been shown to be coordinated by Nuclear factor-erythroid 2-related factor 2 (Nrf2) (Kerins and Ooi, 2017), which is reported to protect from short term iron-induced injury in PTECs. Nrf2 knockout mice showed increased PTEC injury and urinary excretion of NAG 24 h after a single ferric nitrilotriacetate (Fe-NTA) injection (Tanaka et al., 2008). In animal models of chronic kidney disease, Nrf2 activity exhausted over time despite continuous presence of oxidative stress (Aminzadeh et al., 2012; Kim and Vaziri, 2010; Kim et al., 2011). Therefore, we tested the hypothesis that Nrf2 exhaustion as a result of persistent oxidative stress underlies renal injury observed in chronic iron overload conditions.

To this end, we examined the intracellular effects of long-term iron overload exposure in human conditionally immortalized PTECs (ciPTECs) and the role of the Nrf2 pathway herein.

2. Methods

2.1. Cell culture

ciPTECs (clone T1, kindly provided by dr. M. Wilmer, Radboud university medical centre) (Jansen et al., 2014), were cultured using DMEM HAM's F-12 phenol red-free medium (Thermo Fisher Scientific) containing 5 µg/ml insulin, 5 µg/ml transferrin, 5 ng/ml selenium, 36 ng/ml hydrocortisone, 10 ng/ml epithelial growth factor and 40 pg/ml triiodothyronine (all Sigma Aldrich), 10% (v/v) fetal calf serum (Greiner Bio-one), and 1% (v/v) penicillin-streptomycin (Thermo Fisher Scientific). Cells were cultured at 33 °C and 5% CO_2, and grown for 24 h at 33 °C and 5% CO_2 and 7 days at 37 °C and 5% CO_2 prior to experiments.

2.2. Iron exposure

Cells were exposed to 0–500 µM ferric citrate (FeC, Sigma Aldrich) for 72 h (toxicity array) or 48 h (all other experiments) with or without 1 µM trigonelline hydrochloride (Sigma Aldrich).). We calculated that already 100 µM FeC could saturate transferrin levels in fetal calf serum (Young and Garner, 1990) with iron and, as such, this would result in ciPTEC iron exposure containing both saturated TBI and NTBI. Cell pellets were collected and stored at −80 °C until analysis.

2.3. Protein isolation and immunoblotting

Cell pellets were lysed using RIPA buffer (0.15 M NaCl, 0.012 M Sodium Deoxycholate, 0.1% NP40, 0.1% SDS, 0.05 M Tris, pH 7.5, freshly supplemented with protease inhibitors (Complete mini, Roche)). Protein concentration was determined using the Pierce BCA assay kit according to the manufacturer's instructions (Thermo Fisher Scientific). Protein samples were separated on SDS-PAGE gels, transferred to nitrocellulose membrane and incubated with primary antibody overnight at 4 °C. After 1 h incubation at RT with secondary antibody, proteins were visualized on a LAS-3000 scanner for chemiluminescence (Transferrin receptor 1 (TfR1)) or Odyssey fluorescence scanner (all other proteins). Primary antibodies and dilutions are summarized in Supplementary Table 1.

2.4. Nucleus enrichment

Cells were resuspended in mild lysis buffer (10 mM NaCl, 1.5 mM $MgCl_2$, 0.2 mM EDTA, 270 mM sucrose, 0.1% NP-40, 20 mM Tris − HCl, pH 7.5, freshly supplemented with 1 mM DTT and protease inhibitors) and disrupted using a Douncer homogenizer. After centrifugation, pellets were incubated with RIPA lysis buffer and supernatant was collected as nuclear fraction.

2.5. RNA isolation and quantitative PCR

RNA isolation was performed using TRIzol™ (Thermo Fisher Scientific) according to the manufacturer's instructions. A reverse transcription reaction was performed with 1 µg RNA, 4 µl first strand buffer, 1 µl dNTPs (12.5 mM), 2.04 µl random primers, 2 µl DDT, 1 µl M-MLV (all Thermo Fisher Scientific) and 0.5 µl RNAsin (Promega Corporation). The PCR cycle existed of 20 °C for 10 min, 42 °C for 45 min and 95 °C for 10 min. Quantitative PCR was performed on a CFX96 (Bio-rad) using 4 µl cDNA (10 ng/ml), 10 µl SYBR Green Power master mix (Applied Biosystems) and 6 µl primer mix (containing 1 µM forward primer and reverse primer). The PCR protocol was as follows: 7 min at 95 °C, 40 cycles of 15 s at 95 °C and 1 min at 60 °C, and 10 min at 95 °C, with a measurement at the end of each cycle. Fold change values were calculated relative to the housekeeping gene hypoxanthine-guanine phosphoribosyltransferase (HPRT) using the ΔΔCt formula. Primers are summarized in Supplementary Table 2.

2.6. Toxicity array

The RT^2 Profiler PCR Array Human Stress & Toxicity Pathway Finder (Qiagen), containing 84 different genes and 5 housekeeping genes was used together with RT^2 SYBR Green qPCR Mastermix (Qiagen) according to the manufacturer's instructions.

2.7. Iron assessment

Intracellular iron level were determined using the chromogen bathophenanthroline as described (Torrance and Bothwell, 1968). Iron concentrations were calculated by comparison to a standard curve of ferrous sulfate and corrected for protein concentration.

2.8. Oxidative stress measurement

Cells were incubated with 10 µM 2′, 7′-dichlorodihydrofluorescein di-acetate (CM-H_2DCFDA, Thermo Fisher Scientific) and FeC for 1 h at 37 °C. Fluorescence was measured using a Victor X Multilabel Plate Reader (Perkin Elmer).

For oxidative stress staining, cells were incubated with 50 µM CellROX™ Green for 30 min at 37 °C, fixed with 4% paraformaldehyde, stained with DAPI (4′,6-diamidino-2-phenylindole, 300 µM, Thermo Fisher Scientific) and mounted. Images were taken using a Zeiss Apotome FL microscope and AxioVision software.

2.9. Statistical analysis

Data were statistically analyzed using GraphPad Prism 5.03 and presented as mean ± SEM. Results were analyzed by One-Way ANOVA with Dunnett's post test or Student's t-test, where appropriate. Differences were considered statistically significant when $p < 0.05$.

3. Results

3.1. Long term iron overload results in Nrf2 pathway activation

In ciPTECs, 48 h iron overload exposure significantly and concentration-dependently increased intracellular iron levels ($p < 0.05$ for 100 µM and 200 µM, $p < 0.001$ for 500 µM FeC compared to control) (Fig. 1a). High intracellular iron levels are known to decrease TfR1 and induce ferritin protein expression as a result of

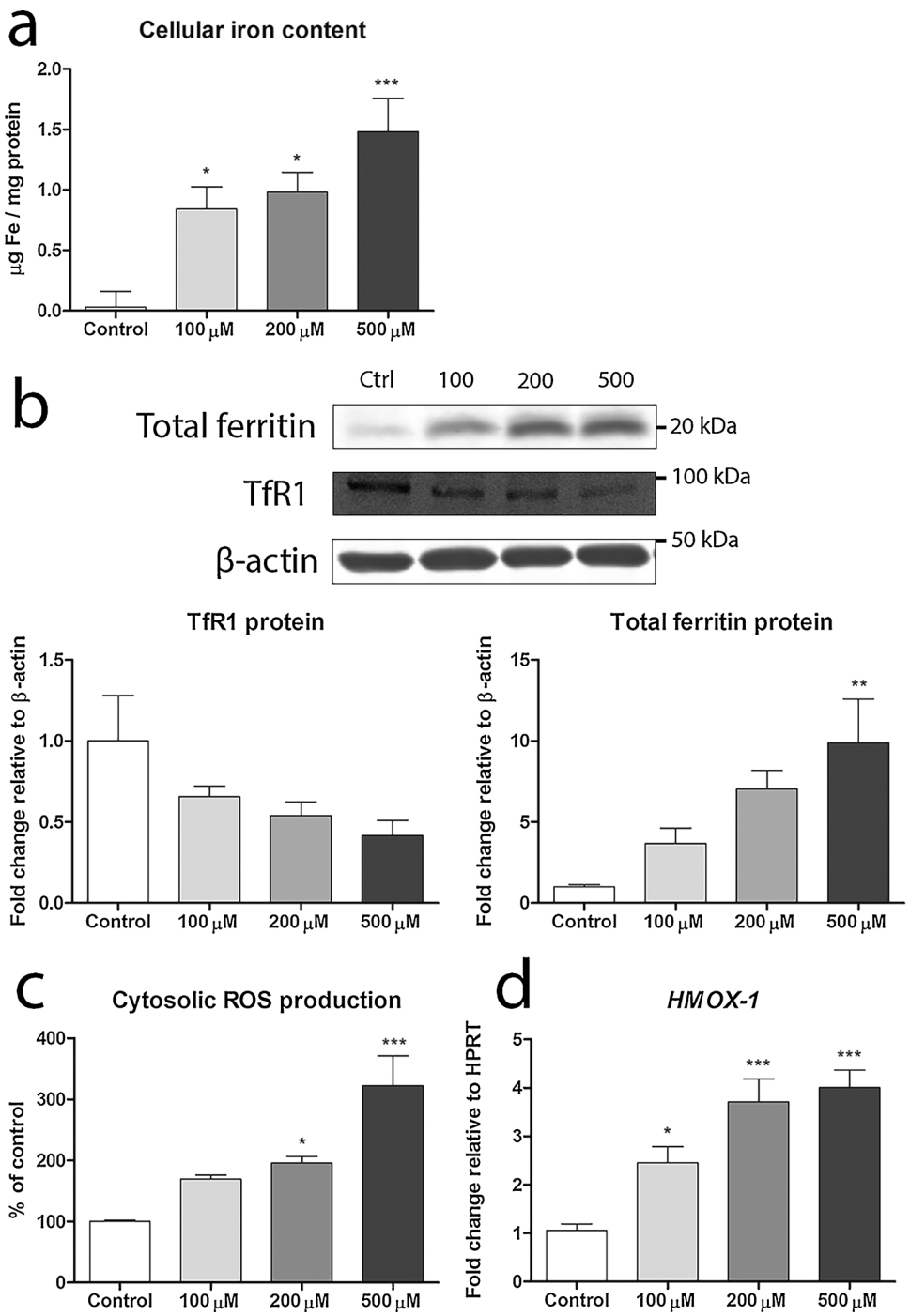

Fig. 1. Long-term iron uptake and resulting cellular stress in ciPTECs.
Intracellular iron concentration (a), total ferritin and transferrin receptor 1 (TfR1) protein levels (b), cytosolic reactive oxygen species (ROS) production (c) and heme oxygenase 1 (*HMOX-1*) mRNA expression after incubation with different concentrations of ferric citrate. Protein content relative to β-actin. Representative images and graphs showing mean of at least three independent experiments. * $p < 0.05$; ** $p < 0.01$; *** $p < 0.001$.

posttranslational genomic iron responsive element – iron responsive protein (IRE-IRP) regulation (Muckenthaler et al., 2017), which was confirmed in our model in a concentration-dependent manner (Fig. 1b). Although morphological cell death was not observed (data not shown), chronic iron exposure significantly induced ROS production ($p < 0.05$ for 200 µM, $p < 0.001$ for 500 µM; Fig. 1c) and *heme oxygenase 1 (HMOX-1)* mRNA expression ($p < 0.05$ for 100 µM, $p < 0.01$ for 200 µM and 500 µM), which is a marker for cellular oxidative stress (Lever et al., 2016) (Fig. 1d).

Next, we applied an explorative gene expression array to identify pathways involved in long-term iron-induced stress in ciPTECs. Indeed, 72 h iron exposure predominantly induced genes regulated by Nrf2 (Fig. 2), including *NAD(P)H quinone dehydrogenase 1 (NQO1), glutamate-cysteine ligase modifier subunit (GCLM)* and *thioredoxin reductase 1 (TXNRD1)*. Induction of these genes was confirmed by additional quantitative PCR, which showed increased mRNA expression of these genes in a concentration-dependent manner upon 48 h of iron exposure, which was statistically significant at 200 µM and 500 µM FeC (Fig. 3a). Chronic iron exposure induced Nrf2 protein levels in enriched nuclear lysates of ciPTECs, without affecting Nrf2 protein levels in total cell

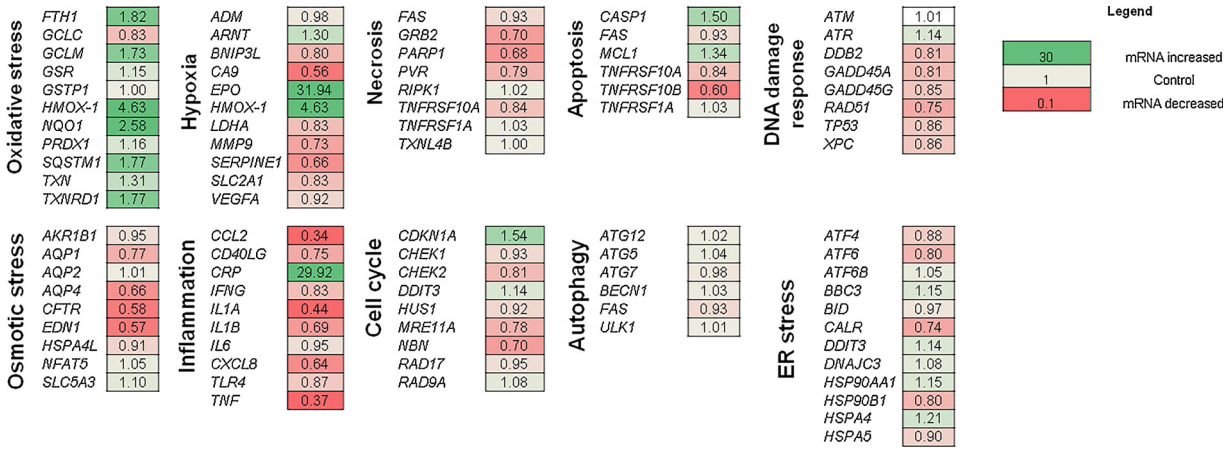

Fig. 2. Explorative qPCR array results after long-term iron overload exposure in ciPTECs.
Results Stress and Toxicity Pathway finder PCR array (Qiagen) after 72 h of exposure to 200 μM ferric citrate compared to control. Genes categorized according to manufacturer's protocol. mRNA expression presented relative to housekeeping gene HPRT. Results indicated as increased (green), similar (grey) or decreased compared to control (red). Description of all genes can be found in Supplementary Table 3.

lysates (Fig. 3b), and moderately increased NQO1 protein levels (Fig. 3c). Together, these data support activation of the Nrf2 pathway by long-term iron exposure.

3.2. Nrf2 downregulation activates other cellular stress mechanisms

To investigate the effects of iron overload exposure upon Nrf2 exhaustion, we used the Nrf2 inhibitor trigonelline to reduce ciPTEC Nrf2 expression (Boettler et al., 2011; Arlt et al., 2013). Addition of trigonelline to iron exposure diminished Nrf2 nuclear translocation, as indicated by significantly reduced Nrf2 protein levels in enriched nuclear lysates whereas Nrf2 protein levels in total cell lysates remained unaffected (Fig. 4a). Moreover, trigonelline also diminished the induction of NQO1 protein levels and decreased mRNA levels of *Kelch like ECH associated protein 1 (KEAP1)*, the Nrf2 binding protein (Kerins and Ooi, 2017) ($p < 0.05$ at 500 μM FeC with trigonelline, compared to 500 μM FeC alone) (Fig. 4b and c, respectively).

Surprisingly, trigonelline co-administration decreased oxidative stress production compared to iron exposure alone (Fig. 5a), whereas *HMOX-1* mRNA levels were not altered (Fig. 5b), indicating that cellular stress was still present. To confirm iron uptake by cells co-incubated with trigonelline, protein levels of TfR1 and ferritin were measured. We again observed a concentration-dependent reduction in TfR1 protein levels (Fig. 5c), similar to previous incubation with iron alone (Fig. 1b), which suggests a comparable intracellular iron content. However, we observed a striking increase in ferritin protein levels in cell exposed to iron and trigonelline compared to iron alone (Fig. 5c). Induction of both ferritin subunits, *H-ferritin* (*FTH*) and *L-ferritin* (*FTL*), was confirmed on mRNA level ($p < 0.05$ for 200 μM and 500 μM iron + trigonelline compared to iron alone for *FTH1;* $p < 0.01$ for 200

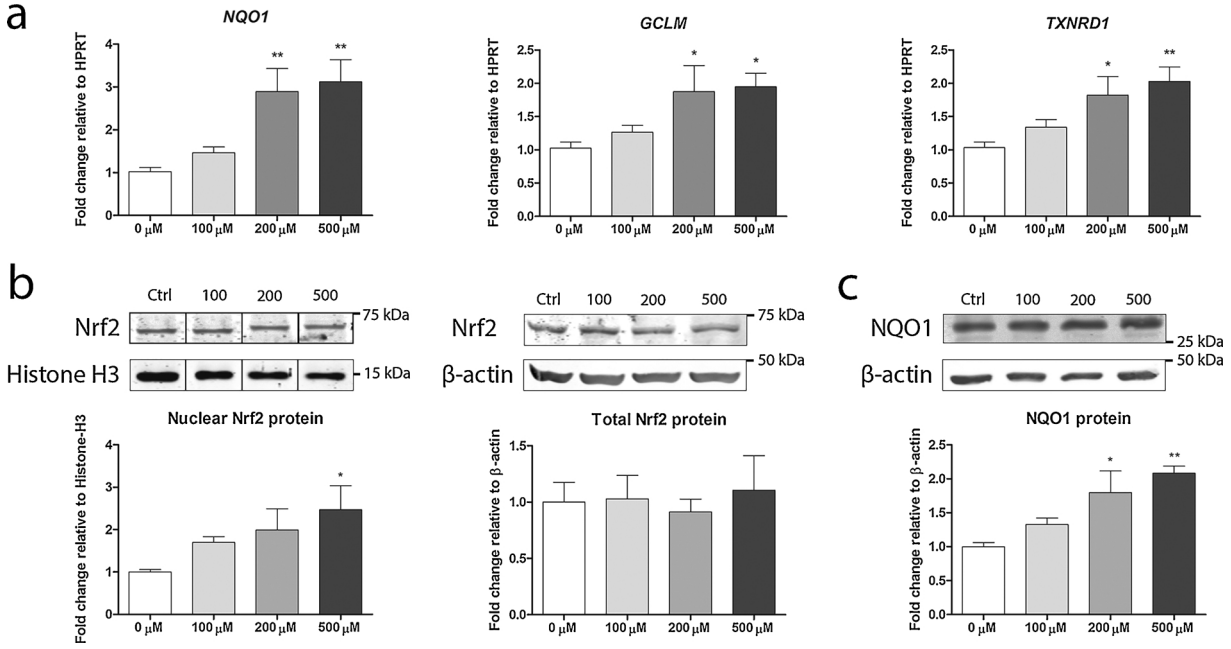

Fig. 3. Nrf2 pathway activation by long-term iron overload in ciPTECs.
NAD(P)H quinone dehydrogenase 1 (NQO1),Glutamate-Cysteine Ligase Modifier Subunit (GCLM) and *Thioredoxin reductase 1 (TXNRD1)* mRNA expression (a), and Nuclear factor erythroid 2-related factor 2 (Nrf2) protein expression in total cell lysate or enriched nuclear fraction, and NQO1 protein expression in total cell lysate (b) after incubation with different concentrations of ferric citrate. Protein content relative to β-actin (total cell lysate) or Histone H3 (nuclear fraction). Representative images and graphs showing mean of at least three independent experiments. * $p < 0.05$; ** $p < 0.01$.

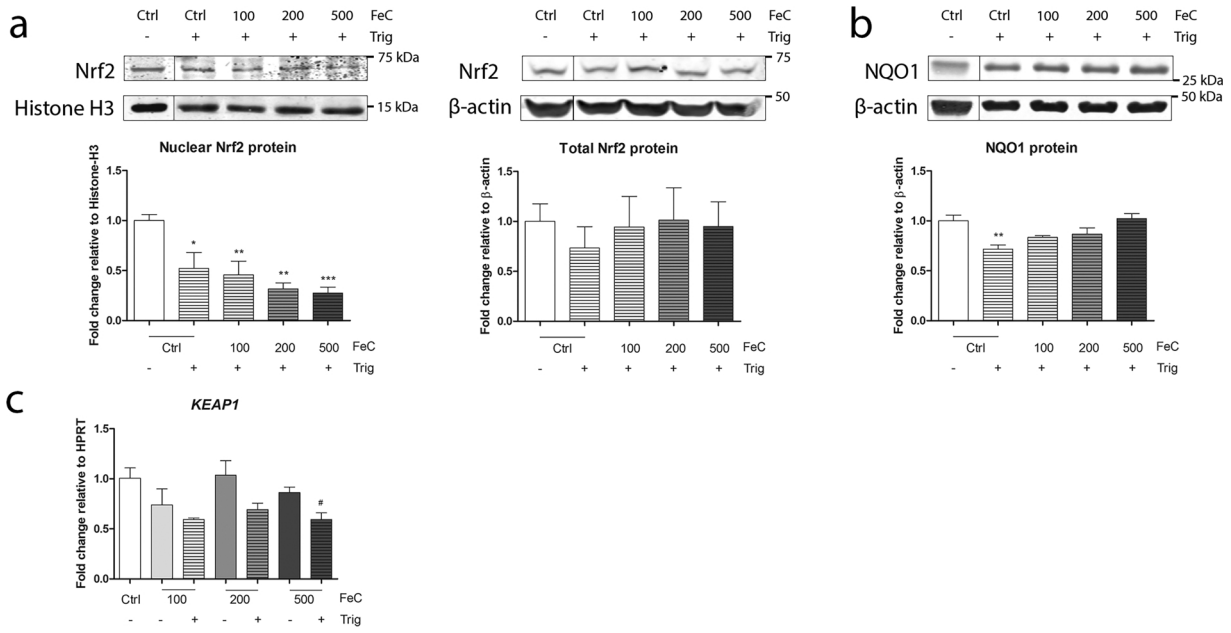

Fig. 4. Nrf2 downregulation using trigonelline in ciPTECs.
Nuclear factor erythroid 2-related factor 2 (Nrf2) protein expression in total cell lysate (a) or enriched nuclear fraction (b), NAD(P)H quinone dehydrogenase 1 (NQO1) protein expression in total cell lysate (c) and *Kelch like ECH associated protein 1 (KEAP1)* mRNA expression after incubation with different concentrations of ferric citrate (FeC) with (striped bars) or without (open bars) the Nrf2 inhibitor trigonelline (Trig). Protein content relative to β-actin (total cell lysate) or Histone H3 (nuclear fraction). Representative images and graphs showing mean of at least three independent experiments. Iron + trigonelline treated cells compared to control, * $p < 0.05$; ** $p < 0.01$; *** $p < 0.001$. Iron + trigonelline treated cells compared to iron only treated cells, $^{\#}$ $p < 0.05$.

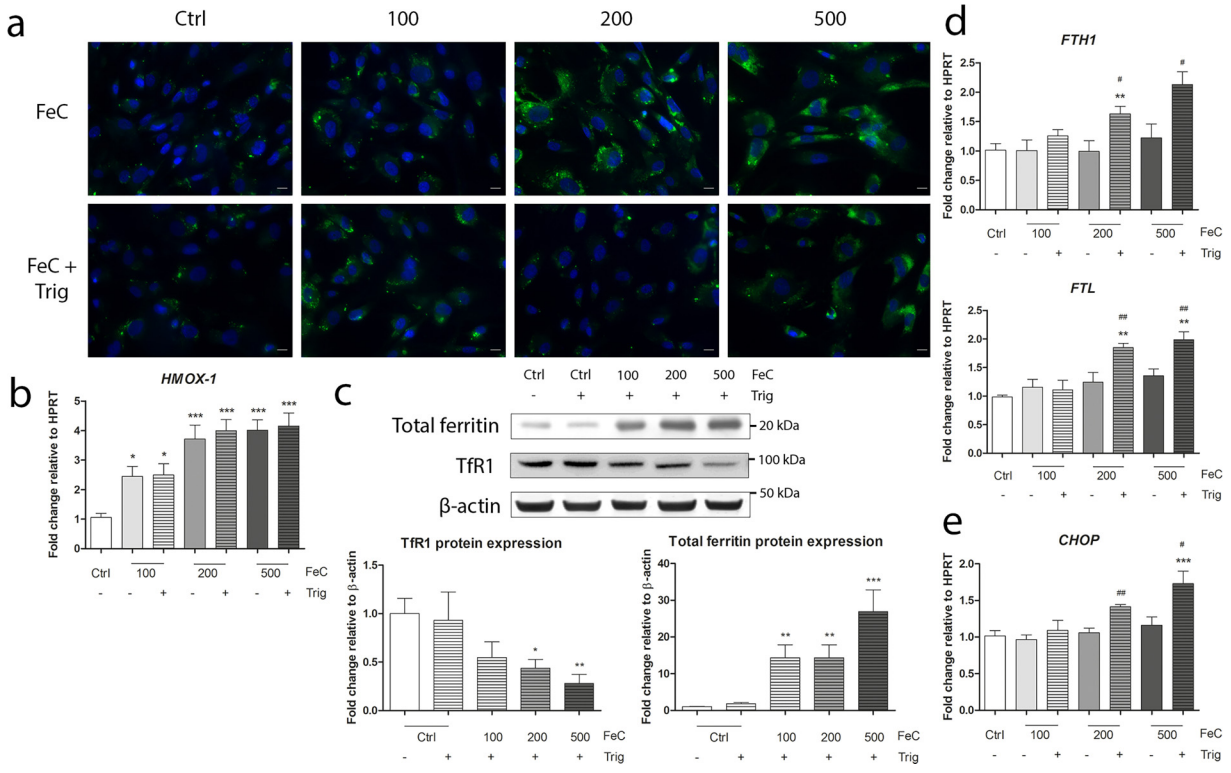

Fig. 5. Nrf2 downregulation shifts cellular stress pathways.
Oxidative stress production (a), *heme oxygenase 1 (HMOX-1)* mRNA expression (b), total ferritin and transferrin receptor 1 (TfR1) protein expression (c), *H-ferritin (FTH1)* and *L-ferritin (FTL)* (d) and *CCAAT-enhancer-binding protein homologous protein (CHOP) mRNA expression* after incubation with different concentrations of ferric citrate (FeC) with (striped bars) or without (open bars) the Nrf2 inhibitor trigonelline (Trig). Protein content relative to β-actin. Representative images and graphs showing mean of at least three independent experiments. Iron + trigoneline treated cells compared to control, * $p < 0.05$; ** $p < 0.01$; *** $p < 0.001$. Iron + trigonelline treated cells compared to iron only treated cells, $^{\#}$ $p < 0.05$; $^{\#\#}$ $p < 0.01$.

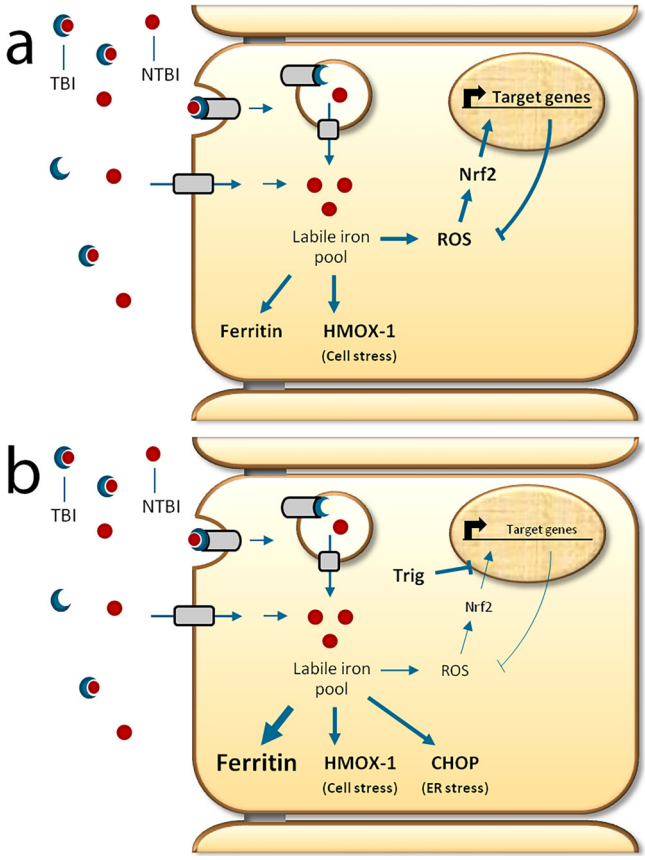

Fig. 6. Schematic overview of stress pathways during long-term iron overload exposure in proximal tubular epithelial cells.
In systemic iron overload, renal tubular epithelial cells are exposed to increased levels of transferrin-bound iron (TBI) and non-transferrin-bound iron (NTBI). Cellular uptake into the labile iron pool results in induction of intracellular iron storage protein ferritin and heme oxygenase 1 (HMOX-1), a marker for cellular stress. Moreover, reactive oxygen species (ROS) are produced, resulting in an anti-oxidative response mediated by Nuclear factor erythroid 2-related factor 2 (Nrf2), balancing oxidative and anti-oxidative conditions (a). When Nrf2 is downregulated by using trigonelline (Trig), ROS production is decreased, whereas HMOX-1 is not affected. Simultaneously, ferritin and CHOP, a marker for endoplasmic reticulum (ER) stress, are induced. This suggests that other stress pathways can be activated during Nrf2 exhaustion, which could potentially mediate chronic iron-induced renal injury (b).

μM and 500 μM iron for *FTL*; Fig. 5d). To explore potential iron-mediated cell stress mechanisms in Nrf2-downregulated cells, we measured CCAAT-enhancer-binding protein homologous protein (CHOP), an indicator of endoplasmic reticulum (ER) stress. We observed a significant induction of *CHOP* mRNA levels with trigonelline co-administration compared to iron alone ($p < 0.05$ for 200 μM iron + trigonelline, $p < 0.01$ for 500 μM iron + trigonelline compared to iron alone, Fig. 5e). This suggests that in case of Nrf2 exhaustion, mechanisms other than oxidative stress may lead to renal injury.

4. Discussion

Chronically increased luminal iron exposure has been associated with renal tubular injury in patients with systemic iron overload. However, the molecular mechanisms involved in injury during chronic iron overload exposure remained unclear. In this study, we showed that long-term iron exposure resulted in iron loading, oxidative cellular stress and activation of the antioxidative protective Nrf2 pathway in ciPTECs. Moreover, Nrf2 downregulation attenuated ROS production, but simultaneously induced *CHOP* and ferritin. This suggests that other stress-related pathways may be activated during persistent iron exposure once the protective Nrf2 pathway is exhausted (Fig. 6).

We showed that long-term iron exposure results in PTEC iron loading, which is in agreement with reports of PT iron deposition in systemic iron overload animal models (Yatmark et al., 2016; Zhou et al., 2000). This resulted in IRE-IRP-mediated downregulation of TfR1 (Muckenthaler et al., 2017), suggesting this transporter may not play a major role in PTEC iron uptake. PTECs have other, presumably IRE-IRP-independent, mechanisms that take up iron during increased luminal iron exposure. Potentially, TBI could be taken up by the endocytic megalin:cubilin transporter complex or divalent metal transporters at the plasma membrane mediate NTBI uptake (Thevenod and Wolff, 2016). Long-term iron exposure activated the antioxidative Nrf2 pathway in ciPTECs. The Nrf2 system is known to protect cells from a large variety of electrophilic and oxidative stressors by coordinating the cellular antioxidant response (Hayes and Dinkova-Kostova, 2014). Indeed, Nrf2 knockout mice are more susceptible to acute Fe-NTA nephrotoxicity than control mice, as shown by enhanced renal tubular necrosis and depletion of glutathione levels in the kidney after Fe-NTA injection (Kanki et al., 2008). We now show that also chronic iron overload activates the antioxidative Nrf2 pathway in vitro. Although we observed increased ROS and cellular stress in ciPTECs after long-term iron exposure, these cells did not show signs of cell death, possibly as a result of Nrf2 activation. Previous studies showed Nrf2 exhaustion in murine models of chronic kidney disease (Aminzadeh et al., 2012; Kim and Vaziri, 2010; Kim et al., 2011). Rats subjected to 5/6 nephrectomy developed oxidative stress and lipid peroxidation over time, whereas Nrf2 protein levels in the remnant kidney tissue were decreased rather than increased compared to control animals (Kim and Vaziri, 2010). Also in Imai rats, a model of spontaneous focal glomerulosclerosis, persistent oxidative stress and impaired Nrf2 activation were observed (Kim et al., 2011). During systemic iron overload, failure of Nrf2 activation could potentiate cytotoxicity of persistent iron overload exposure.

Interestingly, we observed decreased ROS levels, induction of ferritin protein levels and enhanced *CHOP* mRNA levels with Nrf2 downregulation by trigonelline and long-term iron exposure. The iron storage molecule ferritin is mainly regulated by iron availability via IRE-IRP regulation and is increased with intracellular iron loading (Muckenthaler et al., 2017). Increased iron storage in ferritin could prevent intracellular iron from being redox active and could explain our findings of decreased ROS formation (Arosio et al., 2009). In contrast, Nrf2 KO mice showed increased oxidative stress 6 h after Fe-NTA injection (Tanaka et al., 2008; Kanki et al., 2008). This discrepancy could be caused by the iron exposure time, as long-term iron exposure of 48 h in our model could initiate chronic survival mechanisms that differ from acute cellular stress signalling after iron exposure for only 6 h. Potentially, ferritin is not yet increased after 6 h of iron incubation, whereas it is after 48 h, which could explain differential signalling after acute or chronic iron exposure. Ferritin is also induced by inflammatory cytokines and Nuclear Factor kappa-light-chain-enhancer of activated B cell (NF-κB) signalling, the latter being repressed by Nrf2 (Kerins and Ooi, 2017; Pham et al., 2004). Therefore, ferritin induction during Nrf2 exhaustion might involve multiple mechanisms, that require further studies. During Nrf2 inhibition, we observed a shift from oxidative stress to potential ER stress signalling as confirmed by induction of *CHOP* mRNA expression. During long-term ER stress, the physiological unfolded protein response (UPR) becomes overruled by apoptotic UPR signalling, which includes the activation of CHOP and other apoptotic UPR genes (Inagi et al., 2014). In hepatocytes, ER stress activation was reported to induce *H-ferritin* mRNA expression (Oliveira et al., 2009). This suggests that ER stress could also be related to the ferritin induction in ciPTECs during Nrf2 exhaustion. Although ferritin is known to initially safely store iron inside its core, long-term iron accumulation in ferritin shells may be pro-oxidative (Arosio et al., 2009). ER stress in tubular epithelial cells is suggested to be involved in the development

or progression of chronic kidney disease (Inagi et al., 2014). Cells subjected to chronic ER stress are cleared via apoptosis, which is frequently seen in chronic kidney disease (Sanz et al., 2008). Our explorative qPCR array showed that iron overload exposure in ciPTECs induced pro-apoptotic *caspase 1 (CASP1)* but decreased anti-apoptotic *tumor necrosis factor receptor superfamily member 10b (TNFRSF10B)* mRNA expression, suggesting long-term iron exposure may initiate apoptotic cellular signalling. As such, long-term iron overload exposure in patients with systemic iron overload could induce renal PTEC injury through induced ER stress-mediated apoptosis upon intracellular iron accumulation.

In systemic iron overload, PTECs are likely to be a target of iron-mediated injury. Filtered proteins are predominantly reabsorbed by PTECs (Thevenod and Wolff, 2016; Abouhamed et al., 2006), suggesting these cells are exposed to high iron levels in systemic iron overload. Moreover, PTECs are sensitive to injury due to their high level of energy consumption and mitochondrial content (Chevalier, 2016). Nevertheless, in severe iron overload exposure, PTEC injury hampers PTEC iron reabsorption, and increased iron levels pass down the nephron and reach distal tubules. As this could result in iron accumulation and subsequent injury in these epithelial cells, examination of the mechanisms of iron-induced injury in distal tubular epithelial cells is a relevant aspect for future studies.

In conclusion, our findings show that long-term iron exposure activates the Nrf2 pathway in PTECs. Nrf2 exhaustion may result in activation of ER stress and could attribute to chronic iron overload-induced PTEC injury, which may differ from known mechanisms in acute iron-induced kidney injury. Further studies in chronic iron overload models examining the mechanisms of iron-mediated renal injury could be used to identify treatment strategies to decrease iron-mediated renal injury in patients with systemic iron overload.

Conflict of interest statement

Nothing to declare.

Acknowledgements

The authors thank Merel Platenburg and Alex Geerlings for technical assistance.

This work was supported by the Institute for Genetic and Metabolic Disease of the Radboud University Medical Center (2014–2018).

Appendix A. Supplementary data

Supplementary material related to this article can be found, in the online version, at doi:https://doi.org/10.1016/j.toxlet.2018.06.1218.

References

Abouhamed, M., et al., 2006. Divalent metal transporter 1 in the kidney proximal tubule is expressed in late endosomes/lysosomal membranes: implications for renal handling of protein-metal complexes. Am. J. Physiol. Ren. Physiol. 290 (6), F1525–F15333.

Ahmadzadeh, A., et al., 2011. Renal tubular dysfunction in pediatric patients with beta-thalassemia major. Saudi J. Kidney Dis. Transpl. 22 (3), 497–500.

Aminzadeh, M.A., Sato, T., Vaziri, N.D., 2012. Participation of endoplasmic reticulum stress in the pathogenesis of spontaneous glomerulosclerosis–role of intra-renal angiotensin system. Transl. Res. 160 (4), 309–318.

Annayev, A., et al., 2018. Glomerular and tubular functions in children and adults with transfusion-dependent thalassemia. Turk. J. Haematol. 35 (1), 66–70.

Ansar, S., Iqbal, M., AlJameil, N., 2014. Diallyl sulphide, a component of garlic, abrogates ferric nitrilotriacetate-induced oxidative stress and renal damage in rats. Hum. Exp. Toxicol. 33 (12), 1209–1216.

Arlt, A., et al., 2013. Inhibition of the Nrf2 transcription factor by the alkaloid trigonelline renders pancreatic cancer cells more susceptible to apoptosis through decreased proteasomal gene expression and proteasome activity. Oncogene 32 (40), 4825–4835.

Arosio, P., Ingrassia, R., Cavadini, P., 2009. Ferritins: a family of molecules for iron storage, antioxidation and more. Biochim. Biophys. Acta 1790 (7), 589–599.

Boettler, U., et al., 2011. Coffee constituents as modulators of Nrf2 nuclear translocation and ARE (EpRE)-dependent gene expression. J. Nutr. Biochem. 22 (5), 426–440.

Brissot, P., Loreal, O., 2016. Iron metabolism and related genetic diseases: a cleared land, keeping mysteries. J. Hepatol. 64 (2), 505–515.

Brissot, P., et al., 2012. Non-transferrin bound iron: a key role in iron overload and iron toxicity. Biochim. Biophys. Acta 1820 (3), 403–410.

Budak, H., et al., 2014. Stimulation of gene expression and activity of antioxidant related enzyme in sprague Dawley rat kidney induced by long-term iron toxicity. Comp. Biochem. Physiol. C Toxicol. Pharmacol. 166, 44–50.

Cabantchik, Z.I., 2014. Labile iron in cells and body fluids: physiology, pathology, and pharmacology. Front. Pharmacol. 5, 45.

Chevalier, R.L., 2016. The proximal tubule is the primary target of injury and progression of kidney disease: role of the glomerulotubular junction. Am. J. Physiol. Ren. Physiol. 311 (1), F145–F161.

Chmieliauskas, S., et al., 2017. Autopsy relevance determining hemochromatosis: case report. Medicine (Baltimore) 96 (49), e8788.

de Swart, L., et al., 2016. Second international round robin for the quantification of serum non-transferrin-bound iron and labile plasma iron in patients with iron-overload disorders. Haematologica 101 (1), 38–45.

Deveci, B., et al., 2016. Documentation of renal glomerular and tubular impairment and glomerular hyperfiltration in multitransfused patients with beta thalassemia. Ann. Hematol. 95 (3), 375–381.

ElAlfy, M.S., et al., 2018. Renal iron deposition by magnetic resonance imaging in pediatric beta-thalassemia major patients: relation to renal biomarkers, total body iron and chelation therapy. Eur. J. Radiol. 103, 65–70.

Gholampour, F., et al., 2017. The protective effect of hydroalcoholic extract of ginger (Zingiber officinale Rosc.) against iron-induced functional and histological damages in rat liver and kidney. Avicenna J. Phytomed. 7 (6), 542–553.

Ghone, R.A., et al., 2008. Oxidative stress and disturbance in antioxidant balance in beta thalassemia major. Indian J Clin. Biochem. 23 (4), 337–340.

Green, R., et al., 1968. Body iron excretion in man: a collaborative study. Am. J. Med. 45 (3), 336–353.

Hashemieh, M., et al., 2017. Renal hemosiderosis among Iranian transfusion dependent beta-Thalassemia major patients. Int. J. Hematol. Oncol. Stem Cell Res. 11 (2), 133–138.

Hayes, J.D., Dinkova-Kostova, A.T., 2014. The Nrf2 regulatory network provides an interface between redox and intermediary metabolism. Trends Biochem. Sci. 39 (4), 199–218.

Inagi, R., Ishimoto, Y., Nangaku, M., 2014. Proteostasis in endoplasmic reticulum–new mechanisms in kidney disease. Nat. Rev. Nephrol. 10 (7), 369–378.

Jansen, J., et al., 2014. A morphological and functional comparison of proximal tubule cell lines established from human urine and kidney tissue. Exp. Cell. Res. 323 (1), 87–99.

Kanki, K., et al., 2008. A possible role of nrf2 in prevention of renal oxidative damage by ferric nitrilotriacetate. Toxicol. Pathol. 36 (2), 353–361.

Kerins, M.J., Ooi, A., 2017. The roles of NRF2 in modulating cellular iron homeostasis. Antioxid. Redox Signal.

Kim, H.J., Vaziri, N.D., 2010. Contribution of impaired Nrf2-Keap1 pathway to oxidative stress and inflammation in chronic renal failure. Am. J. Physiol. Ren. Physiol. 298 (3), F662–F671.

Kim, H.J., et al., 2011. Role of intrarenal angiotensin system activation, oxidative stress, inflammation, and impaired nuclear factor-erythroid-2-related factor 2 activity in the progression of focal glomerulosclerosis. J. Pharmacol. Exp. Ther. 337 (3), 583–590.

Koppenol, W.H., 1993. The centennial of the Fenton reaction. Free Radic. Biol. Med. 15 (6), 645–651.

Lever, J.M., et al., 2016. Heme oxygenase-1 in kidney health and disease. Antioxid. Redox Signal. 25 (3), 165–183.

Marble, A., Bailey, C.C., 1951. Hemochromatosis. Am. J. Med. 11 (5), 590–599.

Muckenthaler, M.U., et al., 2017. A red carpet for iron metabolism. Cell 168 (3), 344–361.

Norden, A.G., et al., 2001. Glomerular protein sieving and implications for renal failure in Fanconi syndrome. Kidney Int. 60 (5), 1885–1892.

Okumura, A., et al., 2002. Nephrogenic diabetes insipidus associated with hemochromatosis. Am. J. Kidney Dis. 40 (2), 403–406.

Oliveira, S.J., et al., 2009. ER stress-inducible factor CHOP affects the expression of hepcidin by modulating C/EBPalpha activity. PLoS One 4 (8), e6618.

Ozkurt, S., et al., 2014. Renal hemosiderosis and rapidly progressive glomerulonephritis associated with primary hemochromatosis. Ren. Fail. 36 (5), 814–816.

Pham, C.G., et al., 2004. Ferritin heavy chain upregulation by NF-kappaB inhibits TNFalpha-induced apoptosis by suppressing reactive oxygen species. Cell 119 (4), 529–542.

Quinn, C.T., et al., 2011. Renal dysfunction in patients with thalassaemia. Br. J. Haematol. 153 (1), 111–117.

Rodriguez, E., Diaz, C., 1995. Iron, copper and zinc levels in urine: relationship to various individual factors. J. Trace Elem. Med. Biol. 9 (4), 200–209.

Rous, P., 1918. Urinary siderosis : hemosiderin granules in the urine as an aid in the diagnosis of pernicious Anemia, hemochromatosis, and other diseases causing siderosis of the kidney. J. Exp. Med. 28 (5), 645–658.

Sanz, A.B., et al., 2008. Mechanisms of renal apoptosis in health and disease. J. Am. Soc. Nephrol. 19 (9), 1634–1642.

Sheerin, N.S., Sacks, S.H., Fogazzi, G.B., 1999. In vitro erythrophagocytosis by renal tubular cells and tubular toxicity by haemoglobin and iron. Nephrol. Dial Transpl. 14 (6), 1391–1397.

Sponsel, H.T., et al., 1996. Effect of iron on renal tubular epithelial cells. Kidney Int. 50 (2), 436–444.

Tanaka, Y., et al., 2008. Coordinated induction of Nrf2 target genes protects against iron nitrilotriacetate (FeNTA)-induced nephrotoxicity. Toxicol. Appl. Pharmacol. 231 (3),

364–373.
Thevenod, F., Wolff, N.A., 2016. Iron transport in the kidney: implications for physiology and cadmium nephrotoxicity. Metallomics 8 (1), 17–42.
Torrance, J.D., Bothwell, T.H., 1968. A simple technique for measuring storage iron concentrations in formalinised liver samples. S. Afr. J. Med. Sci. 33 (1), 9–11.
von Herbay, A., et al., 1994. Low vitamin E content in plasma of patients with alcoholic liver disease, hemochromatosis and wilson's disease. J. Hepatol. 20 (1), 41–46.
Yatmark, P., et al., 2016. Iron distribution and histopathological study of the effects of deferoxamine and deferiprone in the kidneys of iron overloaded beta-thalassemic mice. Exp. Toxicol. Pathol. 68 (8), 427–434.
Young, S.P., Garner, C., 1990. Delivery of iron to human cells by bovine transferrin. Implications for the growth of human cells in vitro. Biochem. J. 265 (2), 587–591.
Zhang, D., Meyron-Holtz, E., Rouault, T.A., 2007. Renal iron metabolism: transferrin iron delivery and the role of iron regulatory proteins. J. Am. Soc. Nephrol. 18 (2), 401–406.
Zhou, X.J., et al., 2000. Association of renal injury with increased oxygen free radical activity and altered nitric oxide metabolism in chronic experimental hemosiderosis. Lab Invest. 80 (12), 1905–1914.